Plasmon Induced Photovoltage and Charge Separation in Citrate-Stabilized Gold Nanoparticles

Xiaomu Wu,* Elizabeth S. Thrall, Haitao Liu, Michael Steigerwald, and Louis Brus

Chemistry Department, Columbia University, New York, New York 10027

Received: March 25, 2010; Revised Manuscript Received: June 14, 2010

The photoelectrochemistry of citrate-stabilized gold nanoparticles on an ITO electrode is studied at low light intensity. Weak cathodic photovoltage develops under visible gold plasmon irradiation. Photovoltage results from adsorbed citrate oxidation by "hot" holes in the irradiated Au. Under identical conditions, Ag nanocrystals give a stronger photovoltage than Au nanocrystals. The photocurrent is linear in light intensity, and a complete citrate monolayer forms on the Au particles above 10^{-6} M aqueous concentration. At strongly oxidizing potentials, a photocurrent peak occurs which may be related to electron photoinjection from Au into the ITO substrate.

Introduction

This article explores the possibility that electronic excitation of colloidal Au particles can initiate charge transfer photochemistry with adsorbed molecules. Normally, metal particles are thought to be not photochemically active because electron−hole recombination in an excited state is extremely fast. We specifically describe the photoelectrochemical behavior of citrate-stabilized Au nanocrystals on an indium tin oxide (ITO) transparent electrode following optical excitation of the Au surface plasmon. Surface plasmons arise from the collective coherent oscillation of the Au conduction electrons. The optically excited metallic polarization of the surface plasmon creates enhanced Mie scattering, the local-field surface enchanced Raman scattering (SERS) effect, and surface molecular photochemistry.[1] Excited plasmons dephase via Landau damping, producing "hot" electrons and holes. These "hot" electron and holes can localize on adsorbed molecules that have energetically accessible molecular orbitals. Such localization can cause irreversible molecular photochemistry that competes with the return of the hot electron or hole into the metal. The related reverse chemical process has also been extensively studied: exothermic molecular reactions on metal surfaces produce "hot" metallic electrons and holes that can be collected in a Schottky diode external circuit.[2−4]

These hot carrier processes can be efficient. Au nanocrystals adsorbed on TiO_2 have been excited in their visible plasmon band in a Grätzel-type photoelectrochemical cell. A 24% incident-photon-to-electron conversion efficiency was reported for Au "hot" electron injection into the TiO_2 conduction band.[5,6] This high yield is facilitated by an interfacial Schottky barrier which drives injected electrons into the TiO_2 bulk. Au has also been shown to facilitate electron transfer from excited sensitizers,[7−11] to promote photocatalytic oxidation of water to dioxygen,[12] and to improve charge transfer at semiconductor/electrolyte interfaces.[13] Enhanced photoconductance due to tunneling of hot electrons generated by the surface plasmon resonance has been observed in mesoporous TiO_2 nanofibers loaded with Au nanoparticles.[14] Surface plasmon resonance induced photocatalytic chemoselective oxidation of alcohols to carbonyl compounds on Au nanoparticle loaded TiO_2 has also been investigated.[15]

We have proposed a photovoltage mechanism for the photoconversion of sodium citrate stabilized, colloidal Ag nanocrystal seeds to large nanoprisms.[16−18] Ag plasmon excitation causes irreversible oxidation of adsorbed citrate anions. Citrate releases CO_2 after electron transfer to a "hot" Ag hole. This process creates cathodic photovoltage on the aqueous colloidal Ag particle, which can then grow by reduction of aqueous Ag^+. Such cathodic photovoltage, under open circuit in an electrochemical cell, was directly observed for citrate-stabilized Ag particles adsorbed on an ITO electrode at excitation light intensities on the order of 10^{-2} W/cm^2.[19] In colloidal studies, light-initiated growth of an Ag shell on an Au core has been observed. This suggests that photovoltage does develop on the citrate-stabilized Au nanoparticles under plasmon irradiation, leading to reduction of aqueous Ag^+, and subsequent deposition of an Ag^0 shell.[20] Very recently, photovoltage and particle growth by aqueous Ag^+ reduction have been reported at far higher light intensities (10^5 W/cm^2) where two-photon photoionization occurs in Au particles.[21]

Au nanoparticles are more stable and less toxic than Ag particles, and for this reason citrate-stabilized Au nanocrystals are used extensively in medical and biological studies.[22] It is important to understand if substantial photovoltage is created under visible irradiation, for photovoltage would change the rates of redox processes involving the Au particle, and thus modify the local biological redox equilibrium. In this work we study photovoltage under low light intensity (10^{-2} W/cm^2) as used in the colloidal photochemistry experiments. Our findings on the hot-carrier photochemistry of Au nanocrystals under low light intensities may have implications for the use of such nanocrystals in biomedical applications.

There are several reasons why hot carrier chemical processes in Ag and Au nanocrystals could be quite different. Au nanocrystals have a lower plasmon optical excitation cross section, and a larger work function, than Ag nanocrystals. In the optical excitation of Au metal at 514 nm wavelength, the photon energy principally creates d band hot holes.[23] In contrast, in Ag the photon principally creates sp band hot electrons and holes; the d band is not accessible.[23] Thus, the rate and type of photochemistry might be quite different. Recent careful studies

* To whom correspondence should be addressed. E-mail: xw2130@columbia.edu.

10.1021/jp102720r
Published on Web 07/12/2010

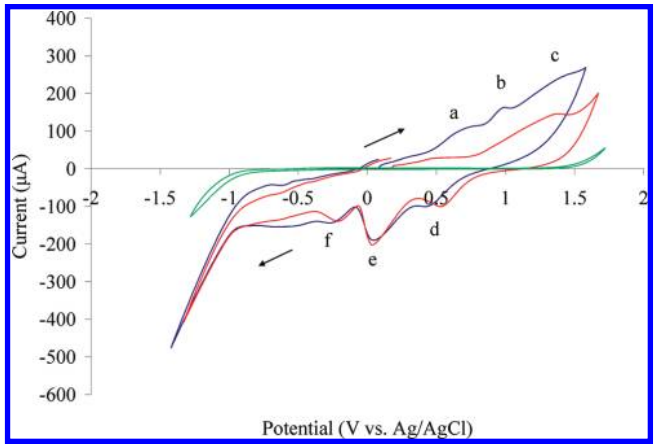

Figure 1. Cyclic voltammograms of an Au particle electrode in 0.5 mM sodium citrate plus 0.1 M KNO_3 (blue), an Au particle electrode in 0.1 M KNO_3 (red), and a bare ITO electrode in 0.5 mM sodium citrate plus 0.1 M KNO_3 (green) under 514 nm illumination (11 mW/cm^2). Sweep speed was 50 mV/s.

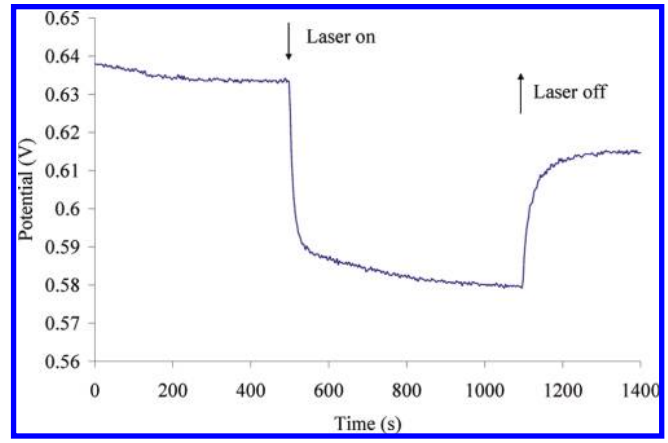

Figure 2. Time trace of open-circuit potential of an Au particle working electrode in an aqueous solution containing 0.5 mM sodium citrate and 0.1 M KNO_3. The laser power was 18 mW/cm^2.

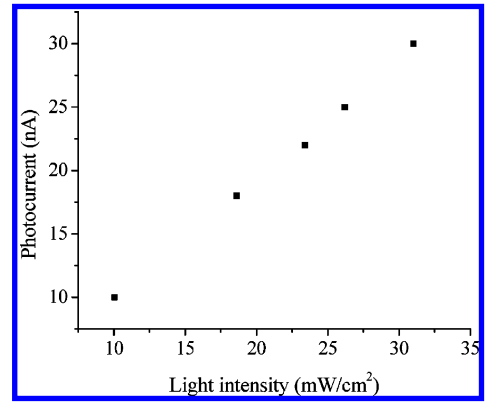

Figure 3. Closed-circuit photocurrent of an Au particle electrode in 0.5 mM sodium citrate and 0.1 M KNO_3 plotted as a function of laser intensity under 514 nm irradiation.

show that the photoisomerization of azobenzene, adsorbed on flat Au in high vacuum, is initiated by transfer of an equilibrated hot hole at the bottom of the d band, lying 2.0 eV below the Au Fermi energy, into the molecular HOMO.[24] In contrast, azobenzene photoisomerization is not observed on flat Ag surfaces, consistent with the idea that hot carrier processes are less important when the d band is not accessible.

Despite this evidence for the importance of d-band accessibility in hot carrier photochemistry of Ag and Au, the situation appears to be reversed for the oxidation of adsorbed citrate. As mentioned above, a strong photovoltage is observed for citrate-stabilized Ag nanocrystals on ITO. This result signifies that a hot carrier process, the photooxidation of citrate, can occur despite the inaccessibility of the Ag d bands. In this work, we explore this photochemical reaction for Au nanocrystals on ITO, and we show that a photovoltage does develop under visible light irradiation, although the response is much weaker. Additionally, we discover a resonant increase in photocurrent at oxidizing potentials that are inaccessible for Ag. These contrasting experiments illustrate that our understanding of these metal-initiated photochemical processes remains unsettled.

Experimental Methods

In a typical experiment, a 3 cm^2 area working Au nanoparticle electrode was made by thermal or electron-beam evaporation of approximately 3 nm of Au onto an ITO-coated glass slide. The doped ITO free carrier concentration is in the range $10^{19}-10^{21}$ cm^{-3}.[25] The electrode was annealed in air at 600 °C for 1 h; this forms well-shaped nanoparticles with a radius around 20 nm and a surface plasmon resonance (SPR) peak at 600 nm (Figures S1 and S2 in the Supporting Information). Photoelectrochemical experiments were run with 514 nm laser illumination. A platinum wire served as the counter electrode, and an Ag/AgCl electrode (in 3 M NaCl) was the reference electrode. The solution was degassed before electrochemical experiments but left open to air during measurements. Specific experimental conditions are given in the figure captions.

Results

The normal cyclic voltammogram (CV) for bare ITO alone in aqueous sodium citrate and KNO_3 is essentially flat (Figure 1, green). The Au-on-ITO electrode CV (Figure 1, blue, red) shows overlapping oxidation waves of several species. Citrate adsorbed on Au oxidizes near 1.0 V vs Ag/AgCl (peak b). Near 1.4−1.5 V Au metal itself oxidizes to Au_2O_3 (peak c); this peak overlaps the peaks due to oxidation of H_2O and acetone dicarboxylic acid.[26−31] The wave at 0.6−0.7 V (peak a) may be due to Au surface oxidation forming chemisorbed species (Au−O).[32] The cathodic peaks (upon return) are attributed to the reductions of gold oxide or surface adsorbate at 0.5 V (peak d), aqueous oxygen at 0 V (peak e), and nitrate ions at −0.2 V (peak f), respectively.[26,33−35] These CVs were taken under an illumination intensity of 11 mW/cm^2; the CVs without illumination essentially superimpose on these traces at this 10^{-4} A current scale. The photocurrent is observed on the 10^{-7} A current scale as described below.

The open-circuit photovoltage of the Au particle electrode is several tens of millivolts under 514 nm irradiation with an intensity of 10−30 mW/cm^2 (Figure 2); this is about 1 order of magnitude lower than the photovoltage of the Ag particle electrode.[19,36] The photocurrent (Figure 3) measured at the rest potential of the particle electrode (closed circuit) is linearly dependent on the illumination intensity at 514 nm. A control experiment shows that the closed-circuit photocurrent for a bare ITO electrode is 1−2 orders of magnitude lower under the same irradiation condition. The photocurrent density at the rest potential is about 9×10^{-10} A/(mW·cm^{-2}); this value is calculated from the slope of photocurrent versus light intensity. Using the dry electrode optical extinction coefficient, this corresponds to a quantum yield of about 3.3×10^{-6} e$^-$/photon. This value is 20-fold lower than the previous result for the Ag particle electrode (6.3×10^{-5} e$^-$/photon).[19]

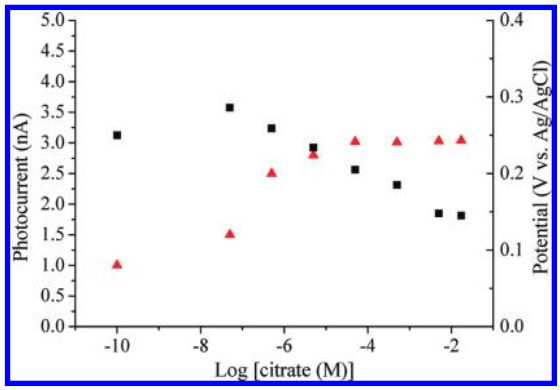

Figure 4. Semilog plot of the closed-circuit photocurrent (red triangles) and rest potential (black squares) of an Au particle electrode, as a function of citrate concentration in aqueous KNO_3 solutions. For each point the KNO_3 concentration was adjusted near 0.1 M to keep the ionic strength constant. The laser power was 14 mW/cm^2.

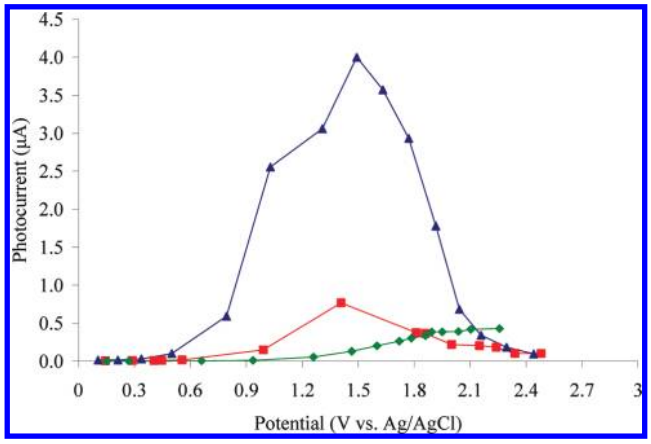

Figure 5. Photocurrent of an Au particle electrode in 0.5 mM sodium citrate and 0.1 M KNO_3 (blue triangles), of an Au particle electrode in 0.1 M KNO_3 (red squares), and of an annealed bare ITO in 0.5 mM sodium citrate and 0.1 M KNO_3 (green diamonds) at different potentials vs Ag/AgCl. The laser intensity was 11 mW/cm^2. The voltage was increased stepwise to higher values.

The closed-circuit photocurrent of the Au nanoparticle electrode increases by about a factor of 3, above the background level observed in KNO_3 electrolyte, when the citrate concentration is increased (Figure 4). The fact that such a modest increase is seen also shows that photooxidation of citrate is weak. The photocurrent saturates at 10^{-6} M citrate with 20 mL of electrolyte in the cell, and we conclude there is a complete citrate monolayer on the Au particles above this concentration. The adsorption of citrate on Au surface lowers the open-circuit potential of the particle electrode.

The dependence of the photocurrent on the applied potential is plotted in Figure 5 (note that the current scale is 3 orders of magnitude lower than in Figure 1). In an electrolyte consisting of KNO_3 and sodium citrate, a maximum value of 3.5×10^{-7} A/(mW$\cdot$cm^{-2}) is observed at 1.5 V vs Ag/AgCl. A shoulder peak is visible at 1.0 V vs Ag/AgCl, with a photocurrent density of 2.3×10^{-7} A/(mW$\cdot$cm^{-2}). For an electrolyte containing KNO_3 alone, a maximum photocurrent density of 6.7×10^{-8} A/(mW$\cdot$cm^{-2}) at 1.4 V vs Ag/AgCl is detected. We correlate the optimum potentials to the onset of the oxidation of citrate, H_2O, and acetone dicarboxylic acid. It is worth pointing out that, in both cases, the photocurrent of the Au particle electrode starts rising drastically at around 0.7 V vs Ag/AgCl, which coincides with the incipient oxidation of Au. This implies that the formation of chemisorbed species (Au−O) may play a role in the photoactivity of Au particles.[32] Nonetheless, no apparent change was found in consecutive closed-circuit photocurrent measurements for over several hours, suggesting that oxidation of Au to Au_2O_3 or $Au(OH)_3$ does not contribute significantly.[5]

Discussion

The photocurrent and photovoltage observed for citrate-stabilized Au particles are weak, on an ITO electrode at potentials near 0 V, in comparison with Ag particles under identical conditions. Less oxidizing potentials (near 0 V) are characteristic of citrate-stabilized, aqueous metallic Au colloidal particles. On ITO we observe that a few tens of millivolts of open-circuit photovoltage develops, and this provides a possible mechanism for the photoreduction of aqueous Ag^+ on aqueous colloidal Au particle core under plasmon irradiation.

We find weak photooxidation of citrate despite the fact that the Au "hot" hole should be strongly oxidizing in comparison with the Ag "hot" hole. The work function of Au (5.3 eV) is 0.7 eV larger than that of Ag (4.6 eV). The equilibrated d band Au "hot" hole lies 2 eV below the Au Fermi level. We conjecture this may be so deep that oxidation of citrate is in the Marcus inverted region, and therefore it is slow.

There are also other factors that will affect the measured photovoltage in Au as compared with Ag. In general, the plasmon metallic polarization is weaker in Au because the excited polarization decays faster than in Ag.[37,38] The 514 nm light is off-resonant with the red Au plasmon peak. It may also be that the specific binding of citrate to the metallic Au surface is different than on Ag,[39−41] in a way that creates stronger coupling of the plasmon to citrate in Ag.

We do observe a pronounced photocurrent peak under strongly oxidizing conditions near 1.0 V; however, at this potential both Au and citrate are undergoing rapid normal electrochemical (dark) oxidation. This behavior is remarkably different from the behavior of fullerene-modified bulk Au[42] or bare ITO electrodes, where photocurrent saturates with increasing positive bias. This 10^{-7} A level photocurrent peak in the presence of citrate under strongly oxidizing conditions may be related to electron photoinjection from Au into ITO. The ITO substrate is a heavily doped semiconductor with a band gap of 3.6 eV. An interfacial Schottky barrier may form at the ITO/Au junction, as previously observed on TiO_2.[43] This barrier would drive photoinjected electrons from Au into the high density of states in the ITO conduction band. At oxidizing potentials, such hot electron photoinjection could occur in parallel to the direct tunneling of thermalized electrons from the Au Fermi level to the ITO. This direct tunneling current results from the oxidation of citrate by holes at the Au Fermi level, and from the oxidation of Au itself, at potentials near 1.0 V. These oxidation processes occur in the absence of photoexcitation. As the CVs show, direct electron tunneling occurs on the 10^{-4} A level at 1.0 V, far exceeding the 10^{-7} A level photocurrent at the same potential.

Conclusions

In conclusion, we present the direct measurement of plasmon mediated charge separation in citrate-stabilized Au nanoparticles on an ITO-coated substrate, at low light intensities characteristic of colloidal photochemical growth experiments. The process is linear in light intensity, and a few tens of millivolts of photovoltage develops. At 514 nm excitation wavelength photooxidation of citrate is weak in comparison with Ag particles under identical conditions. At more oxidizing potentials, we observe a stronger photocurrent which may be associated

with photoinjection of electrons from Au into the ITO conduction band. Unlike the Ag particle electrode, no degradation or corrosion of Au particles is observed.

Acknowledgment. This work was supported by the DOE Basic Energy Sciences program under FG02-98ER14861. It was also partially supported by the Nanoscale Science and Engineering Initiative of the NSF under Award No. CHE-0641523 and by the New York State Office of Science, Technology, and Academic Research (NYSTAR). We have used characterization facilities supported by the Columbia MRSEC under NSF Award No. DMR-02113574.

Supporting Information Available: UV−vis spectra and SEM images of a typical Au particle electrode. This material is available free of charge via the Internet at http://pubs.acs.org.

References and Notes

(1) Brus, L. *Acc. Chem. Res.* **2008**, *41*, 1742.
(2) Huisman, E. H.; Guedon, C. M.; van Wees, B. J.; van der Molen, S. J. *Nano Lett.* **2009**, *9*, 3909.
(3) Hervier, A.; Renzas, J. R.; Park, J. Y.; Somorjai, G. A. *Nano Lett.* **2009**, *9*, 3930.
(4) Nienhaus, H. *Surf. Sci. Rep.* **2002**, *45*, 1.
(5) Tian, Y.; Tatsuma, T. *J. Am. Chem. Soc.* **2005**, *127*, 7632.
(6) Sakai, N.; Fujiwara, Y.; Takahashi, Y.; Tatsuma, T. *ChemPhysChem* **2009**, *10*, 766.
(7) Kamat, P. V. *J. Phys. Chem. B* **2002**, *106*, 7729.
(8) Imahori, H.; Norieda, H.; Yamada, H.; Nishimura, Y.; Yamazaki, I.; Sakata, Y.; Fukuzumi, S. *J. Am. Chem. Soc.* **2001**, *123*, 100.
(9) Hirayama, D.; Takimiya, K.; Aso, Y.; Otsubo, T.; Hasobe, T.; Yamada, H.; Imahori, H.; Fukuzumi, S.; Sakata, Y. *J. Am. Chem. Soc.* **2002**, *124*, 532.
(10) Yamada, H.; Imahori, H.; Nishimura, Y.; Yamazaki, I.; Ahn, T. K.; Kim, S. K.; Kim, D.; Fukuzumi, S. *J. Am. Chem. Soc.* **2003**, *125*, 9129.
(11) Hasobe, T.; Imahori, H.; Kamat, P. V.; Ahn, T. K.; Kim, S. K.; Kim, D.; Fujimoto, A.; Hirakawa, T.; Fukuzumi, S. *J. Am. Chem. Soc.* **2005**, *127*, 1216.
(12) Currao, A.; Reddy, V. R.; Calzaferri, G. *ChemPhysChem* **2004**, *5*, 720.
(13) Subramanian, V.; Wolf, E.; Kamat, P. V. *J. Phys. Chem. B* **2001**, *105*, 11439.
(14) Son, M. S.; Im, J. E.; Wang, K. K.; Oh, S. L.; Kim, Y. R.; Yoo, K. H. *Appl. Phys. Lett.* **2010**, *96*, 023115.
(15) Naya, S.; Inoue, A.; Tada, H. *J. Am. Chem. Soc.* **2010**, *132*, 6292.
(16) Jin, R. C.; Cao, Y. W.; Mirkin, C. A.; Kelly, K. L.; Schatz, G. C.; Zheng, J. G. *Science* **2001**, *294*, 1901.
(17) Jin, R. C.; Cao, Y. C.; Hao, E. C.; Metraux, G. S.; Schatz, G. C.; Mirkin, C. A. *Nature* **2003**, *425*, 487.
(18) Wu, X. M.; Redmond, P. L.; Liu, H. T.; Chen, Y. H.; Steigerwald, M.; Brus, L. *J. Am. Chem. Soc.* **2008**, *130*, 9500.
(19) Redmond, P. L.; Brus, L. E. *J. Phys. Chem. C* **2007**, *111*, 14849.
(20) Xue, C.; Millstone, J. E.; Li, S. Y.; Mirkin, C. A. *Angew. Chem., Int. Ed.* **2007**, *46*, 8436.
(21) Lee, S. J.; Piorek, B. D.; Meinhart, C. D.; Moskovits, M. *Nano Lett.* **2010**, *10*, 1329.
(22) Daniel, M. C.; Astruc, D. *Chem. Rev. (Washington, D.C.)* **2004**, *104*, 293.
(23) Petek, H.; Nagano, H.; Ogawa, S. *Appl. Phys. B* **1999**, *68*, 369.
(24) Hagen, S.; Kate, P.; Leyssner, F.; Nandi, D.; Wolf, M.; Tegeder, P. *J. Chem. Phys.* **2008**, *129*, 164102.
(25) Reddy, V. S.; Das, K.; Dhar, A.; Ray, S. K. *Semicond. Sci. Technol.* **2006**, *21*, 1747.
(26) Chailapakul, O.; Popa, E.; Tai, H.; Sarada, B. V.; Tryk, D. A.; Fujishima, A. *Electrochem. Commun.* **2000**, *2*, 422.
(27) Park, J. E.; Momma, T.; Osaka, T. *Electrochim. Acta* **2007**, *52*, 5914.
(28) Trettenhahn, G.; Koberl, A. *Electrochim. Acta* **2007**, *52*, 2716.
(29) Colucci, J.; Montalvo, V.; Hernandez, R.; Poullet, C. *Electrochim. Acta* **1999**, *44*, 2507.
(30) Kuyper, A. C. *J. Am. Chem. Soc.* **1933**, *55*, 1722.
(31) Shakila, V.; Pandian, K. *J. Solid State Electrochem.* **2007**, *11*, 296.
(32) Watanabe, T.; Gerischer, H. *J. Electroanal. Chem.* **1981**, *122*, 73.
(33) El-Deab, M. S.; Ohsaka, T. *Electrochim. Acta* **2002**, *47*, 4255.
(34) El-Deab, M. S. *Electrochim. Acta* **2004**, *49*, 1639.
(35) Sarapuu, A.; Nurmik, M.; Mandar, H.; Rosental, A.; Laaksonen, T.; Kontturi, K.; Schiffrin, D. J.; Tammeveski, K. *J. Electroanal. Chem.* **2008**, *612*, 78.
(36) Redmond, P. L.; Wu, X. M.; Brus, L. *J. Phys. Chem. C* **2007**, *111*, 8942.
(37) Link, S.; El-Sayed, M. A. *J. Phys. Chem. B* **1999**, *103*, 8410.
(38) Hodak, J. H.; Martini, I.; Hartland, G. V. *J. Phys. Chem. B* **1998**, *102*, 6958.
(39) Kilin, D. S.; Prezhdo, O. V.; Xia, Y. *Chem. Phys. Lett.* **2008**, *458*, 113.
(40) Kunze, J.; Burgess, I.; Nichols, R.; Buess-Herman, C.; Lipkowski, J. *J. Electroanal. Chem.* **2007**, *599*, 147.
(41) Nichols, R. J.; Burgess, I.; Young, K. L.; Zamlynny, V.; Lipkowski, J. *J. Electroanal. Chem.* **2004**, *563*, 33.
(42) Enger, O.; Nuesch, F.; Fibbioli, M.; Echegoyen, L.; Pretsch, E.; Diederich, F. *J. Mater. Chem.* **2000**, *10*, 2231.
(43) McFarland, E. W.; Tang, J. *Nature* **2003**, *421*, 616.

JP102720R